The Cartridge: A Canonical Neural Circuit Abstraction of the Lamina Neuropil Construction and Composition Rules

Neurokernel RFC # 2

Aurel A. Lazar Nikul H. Ukani
Yiyin Zhou *
Department of Electrical Engineering
Columbia University, New York, NY 10027

January 29, 2014

Abstract

The Lamina is a neuropil that resides in the optic lobe of the early visual system of the fruit fly. Its neural circuit consists of some 700 $\sim$ 800 cartridges. A cartridge is an atomic neural circuit abstraction whose I/O behavior can be studied in isolation. The anatomy of the neurons, neurotransmitter types and connectivity patterns of the neurons in the cartridge are briefly reviewed. A circuit-level model of a cartridge suitable for implementation on a GPU platform is presented in detail. Cartridge interconnects create neural circuits with different I/O characteristics. A number of cartridge composition rules for building neural circuits with different spatial I/O characteristics are discussed. We present a model neural circuit for initial functional evaluations and scaling of the Lamina and its interconnection with the Medulla. Implementation considerations of the Lamina neural circuit are discussed.

*Names are listed in alphabetical order.

Contents

1 Introduction

Studies of *Drosophila melanogaster* have revealed that each side of its brain consists of some 50 neuropils [1]. Each neuropil is characterized by spatially restricted local neurons and projection neurons connecting to other neuropils in the fly brain [1]. Called local processing units (LPUs), these modules can be regarded as the key building blocks of the fly brain. Subsystems in the fly brain comprise multiple neuropils interconnected through neural tracts.

The development of the Neurokernel project (`http://neurokernel.github.io`) focuses on modeling and emulating the entire fly brain by identifying LPUs and their interconnects as the fundamental computational building blocks of the brain. The project investigates models of neural computation for the fly brain by (i) constructing models of LPUs arising in sensory systems and motor control of the fly brain, and by (ii) interconnecting constituent LPUs with models of synaptic tracts [2].

Vision is critical for the fly for avoiding predators, flight control, mating, etc.. In order to gain insights into the general principles of neural processing of the fruit fly visual system, we model here the first optic neuropil, the Lamina. Our working hypothesis is that, since the Lamina only contains a very small number of neuron types and has spatially structured neural circuits, by characterizing its I/O behavior it may become possible to uncover some of the information processing transformations that take place in the first stage of visual processing.

The anatomical structure of the Lamina has been studied extensively and most of the cell types have been identified [3]. A recent study mapped out most of the synaptic connections [4] (i.e., chemical synapses). In addition, genetic techniques have helped to identify some of the neurotransmitters in the optic lobe [5, 6, 7, 8]. Moreover, imaging and recordings paired with genetic manipulation has led to the understanding of some of the functional properties of the cells in the Lamina [9].

The objective of this RFC is to combine all the currently available information regarding the Lamina LPU to construct a model that can be used in the Neurokernel environment. Towards this goal, we identify the key components in modeling the neural circuits of the Lamina including (i) cartridges as a canonical neural circuit abstraction, and (ii) composition rules among cartridges [10].

The RFC is organized as follows. In Section 2, we briefly describe the anatomy of the early visual system of the fruit fly. Next, in Section 3, we describe the neuronal components of the Lamina including the neuron types, neurotransmitters and

connectivity among neurons. We then propose in section 4 a model for constructing the Lamina for functional evaluations. In section 5, we present details of the implementation of the proposed Lamina model.

2 Anatomy of the Fly's Early Vision System

The early visual system of the fruit fly resides in the optic lobe. It consists of the Retina and 4 neuropils, namely, the Lamina, the Medulla, the Lobula and the Lobula plate (see Fig. 1). The optic lobe is estimated to comprise more than half of the total numbers of neurons in the fruit fly. The total cell count of the optic lobe on each side of the brain is approximately $66,000$, of which about $5,000$ are in the retina, $6,000$ are in the Lamina, $40,000$ are in the Medulla and $15,000$ are in the Lobula complex [11].

The Lamina sits behind the retina, and is the first of the optic neuropils in the Drosophila's compound eye. The relative position of the Lamina in the optic lobe is shown in Fig. 1. For more details, see [3, 12, 13, 14] and the references therein.

The Lamina receives inputs from six photoreceptors (R1-R6) located in the Retina. Most of the inputs to the next neuropil, the Medulla, are provided by neurons in the Lamina, exceptions being the two color sensitive photoreceptors (R7-R8) that bypass the Lamina. Thus, the first stage of visual processing is performed in the Lamina.

3 Neurons and Neurotransmitters in the Lamina

3.1 Neurons

The Lamina consists of some $6,000$ neurons. They can be categorized into two types of neurons: projection (or output) neurons whose axons project to the Medulla and Local Neurons (LNs) whose interconnects do not project outside of the neuropil. In addition, some of the axons of the photoreceptor cells in the Retina innervate the Lamina. They represent the inputs to this neuropil. We list all the input neurons and the Lamina neurons in the following.

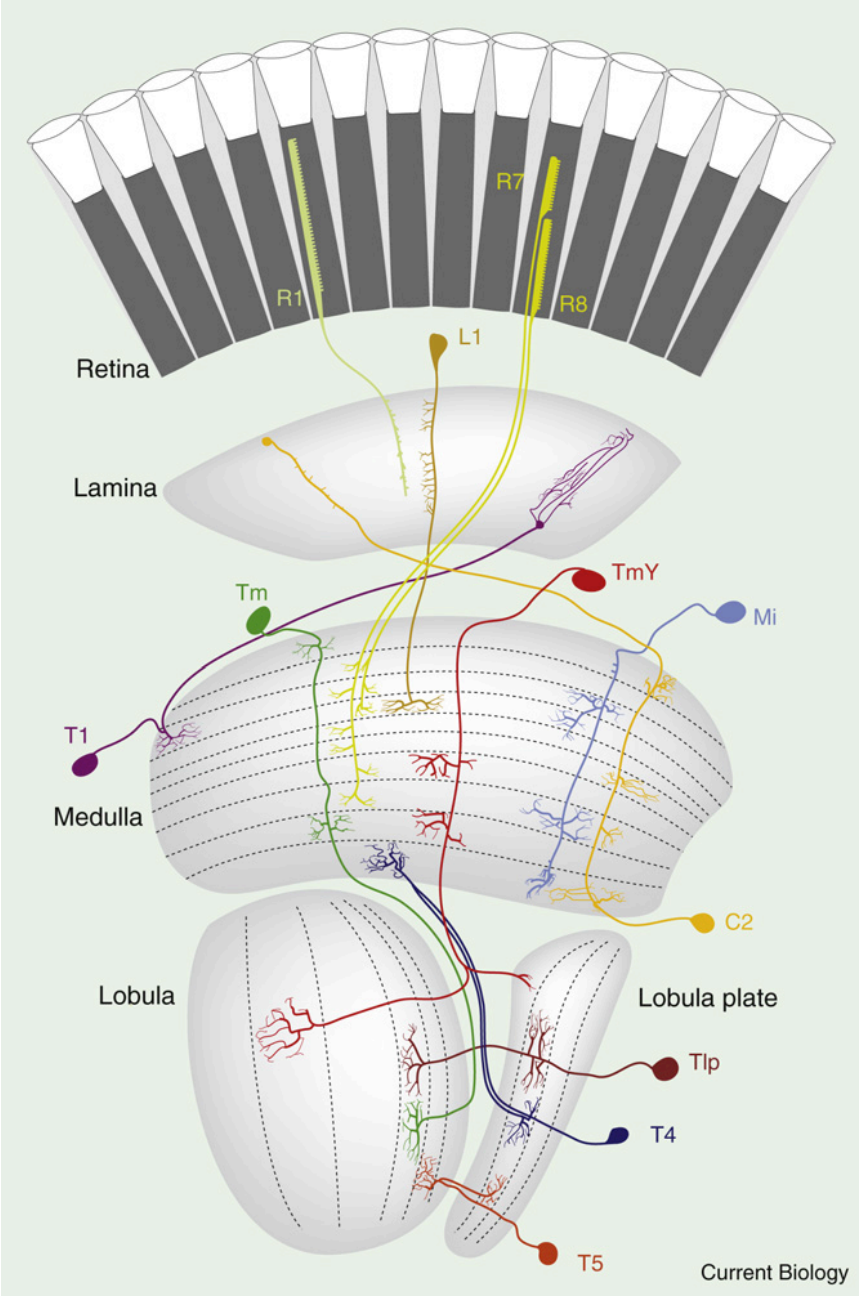

Figure 1: Structure of the optic lobe. The Lamina is the first neuropil behind the Retina and in front of the Medulla. (From [14], Copyright ©Elsevier 2009).

Inputs The inputs to the Lamina consists of some $4,500$ axons of the photoreceptors R1-R6.

Output Neurons Neuron types/classes in the Lamina are typically categorized by their morphology. There are a total of 10 types/classes of output neurons in the Lamina.

The first class of neurons are the *Large Monopolar Cells* (LMCs). Their cell body resides between the Retina and the Lamina neuropil. Unlike many other neurons that have the dendritic tree and axon on separate branches, each of the LMCs only extends a single branch of neurite from their cell body and both dendrites and axon terminals reside on this branch (see Figure 1). The latter configuration is the basis of their names (see also Figure 3 in [3]). The LMCs can be subdivided into 5 types, L1-L5. L1 and L2 have the largest axon diameter while L3 has a medium sized axon while L4 and L5 have relatively much thinner axons. LMCs amount to about $4,000$ neurons in the Lamina. They all terminate in the Medulla [3, 5].

Some 750 T1 cells make up a class on their own. They have bushy arborization in the Medulla and extends thin processes into the Lamina. T1 neurons terminate in the Medulla [3].

The Centrifugal neurons C2 and C3 have their cell bodies between the Medulla and the Lobula complex. Their neurites extend backwards into the Lamina. The Centrifugal neurons amount to $1,500$ cells and they all terminate in the Medulla [3, 5].

The Lamina wide-field (Lawf) neurons are another type of output neurons of the Lamina. Lawf neurons innervate widely in the distal part of the Lamina and terminate in the distal parts of the Medulla (see Figure 3 in [3]).

Lamina Tangential (Lat) neurons arborize widely in the Lamina. However, it is unclear which neuropil they project their axon to [3]. They are presumably only a few in numbers.

Local Neurons Amacrine cells (Am) are the only local neurons. They cover a large spatial field, and send thin processes through adjacent photoreceptor axons. The number of amacrine cells in the Lamina isn't clear yet but it is estimated to be around $200 \sim 400$.

3.2 Neurotransmitters

Neurons in the lamina utilize diverse types of neurotransmitters and receptors. Neurotransmitter released by the pre-synaptic neuron and the receptor expressed by the post-synaptic neuron pair together to define the function of a chemical synapse.

We summarize the neurotransmitter types of neurons in the Lamina in Table 1. The neurotransmitter receptor expressed in each type of neurons are summarized in Table 2.

Table 1: Summary of neurotransmitter release by each neuron type.

Neuron	Neurotransmitter	references	Note
R1-R6	histamine	[15, 13]	
L1	glutamate	[16]	
L2	acetylcholine	[16]	
L3	glutamate	[17]	identified for other fly species
L4	acetylcholine	[16]	
L5	glutamate		hypothetical due to close relation with L1
T1			no data
C2	GABA	[5]	
C3	GABA	[5]	
Am	glutamate	[5]	
Lawf			no data
Lat	serotonin	[3]	

Substantial amount of information about neurotransmitters is still missing. The missing information cannot be revealed by the typical EM reconstruction techniques used in connectomics [20]. We have made educated guesses to complete the tables in order to establish a full configuration for the Lamina. As such information becomes available, more precise synaptic models can be adopted and implemented.

Table 2: Summary of neurotransmitter receptors expressed by each neuron type.

Neuron	Identified Receptors	references	Note
R1-R6	AChR ionotropic glutamate receptor		Consistent with the presynaptic neuron [18, 4]
L1	HCLA	[19]	additional glutamate and GABA receptors possible
L2	HCLA, AChR	[19, 16]	additional GABA receptors possible
L3	HCLA	[19]	additional glutamate and GABA receptors possible
L4	AChR	[16]	
L5	ionotropic glutamate receptor GABA receptor		Consistent with the extensive # of synapses with L1, C2 and C3
T1	NMDA	[17]	identified for other fly species
C2	$GABA_B$	[5]	additional glutamate receptors possible
C3	$GABA_B$	[5]	additional glutamate receptor possible
Am	HCLA	[19]	additional GABA receptor possible
Lawf	$GABA_A$, $GABA_B$	[5]	
Lat			no data

4 Neural Circuit Level Modeling of the Lamina

Modeling the Lamina neural circuit can be decomposed into modeling its some 700 $\sim$ 800 cartridges and the interconnects between them. As such, the cartridge can be considered as an atomic neural circuit abstraction that can be studied in isolation. A set of simple interconnects with well defined rules of cartridge composition enables the construction of more complex circuits including the Lamina itself.

4.1 Cartridges as Canonical Neural Circuit Abstractions

Columnar Structure Similar to the spatially regular structure of the Retina provided by the ommatidia, the Lamina exhibits a columnar structure that preserves the retinotopy. Called cartridges, these columnar units have a one-to-one association with the ommatidia. Retinotopy is preserved since the adjacent ommatidia are associated with adjacent cartridges. In addition, cell types, number of cells and their connections are stereotypic in each cartridge. Thus, a cartridge, can be seen as an instance of a canonical neural circuit abstraction (cNCA) and the function of the Lamina can be largely understood by investigating the neural circuit underlying the cartridge and the composition rules among multiple cartridges [10].

Decomposing the Lamina circuit into cartridges and defining a set of composition rules among them has the following advantages:

- the cartridge as an atomic unit of computation naturally reflects the structural complexity of the anatomy of the Lamina.
- as a single unit, each cartridge performs the processing of a localized retinal input, i.e., a univariate signal.
- the I/O functionality of the cartridge can be studied in isolation. Since the cartridge is a fundamental computational unit, the insights gained about its I/O behavior may have a broader applicability towards understanding brain function.
- cartridge composition rules can be studied using components that are well understood. The processing of multivariate signals can then be achieved by certain composition rules. The modularity of such rules may have been evolutionarily advantageous for spatial scaling of the compound eye.

In light of this discussion, we first model the cartridge as a cNCA and describe its circuit components and their connectivity.

Input The inputs to the Lamina are from the retina photoreceptors. The 6 photoreceptors, R1-R6, that are not color sensitive, terminate in a cartridge. However, none of the 6 photoreceptors belongs to the ommatidium directly associated with the cartridge located immediately "above". In fact, each connection belongs to a different ommatidium adjacent to the associated ommatidium and innervates a cartridge according to the neural superposition rule illustrated Fig. 2 [21, 14]. Fig. 2 shows an overlaid hexagonal grid resembling the organizational structure of the ommatidia (solid circles) and cartridges (dashed circles). The target cartridge A receives inputs from one of the photoreceptors in each of the six ommatidia that are highlighted with individual photoreceptors R1-R6 (black dots) and R7/R8 (green dots). In addition, the right side of Fig. 2 indicates the cartridge that each of the six photoreceptors from a single ommatidium projects to. It is easy to verify that this projection pattern tiles the visual space. That is, each cartridge exactly receives only 6 photoreceptor inputs, each from a different ommatidium. More importantly, all photoreceptors that project to one cartridge share the same optical axis [21]. Therefore, the brightness signal relayed by photoreceptors to a single cartridge comes from parallel rays at a certain angle.

Output The outputs of each cartridge comprise five L1-L5 neurons (LMCs), one T1 neuron and two centrifugal neurons C2 and C3. All of these output neurons innervate and terminate in the Medulla. L1-L3 receive direct photoreceptor inputs, but L4 and L5 requires a second synapse in the Lamina for signals originating in the Retina to reach them. Moreover, L1 is postsynaptic to C3 and L2 is postsynaptic to both C2 and C3 neurons. The majority of the synaptic interactions of the centrifugal neurons C2 and C3 occur in the medulla but they do receive some input from R5 and R3, respectively, in the Lamina. The T1 neurons receive input mainly from the Amacrine cells in addition to some inputs from photoreceptors R2-R4 [4]. In addition, some output neurons, for example, L2 and L4, also feed back their state into the photoreceptor axons [18].

Local Neurons In addition to the 8 output cartridge neurons and 6 input lines, another repetitive element in a cartridge are the α-profiles. These are thin processes (neurites) generated by the tangentially oriented Amacrine cells. The anatomical structure of the Amacrine cell is shown in Fig. 3. On the one hand, each cartridge typically has 6 α-profiles that may come from $1-6$ Amacrine cells [3]. On the other hand, each Amacrine cell may innervate $6-12$ cartridges. Each α-profile goes through the gap between two adjacent photoreceptor axons. They are post-synaptic

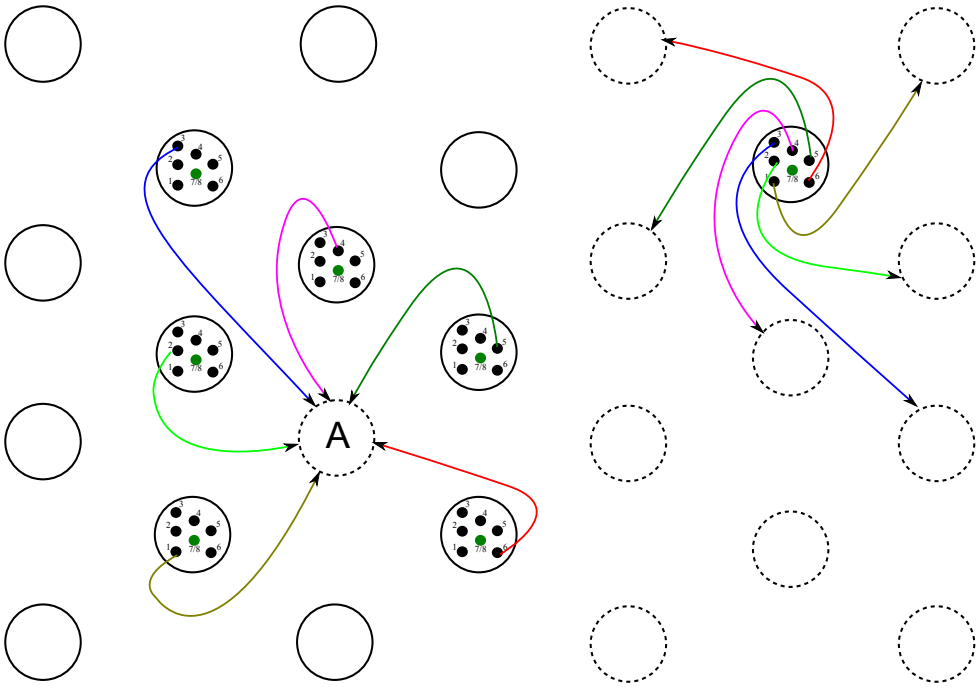

Figure 2: Neural superposition rule of the fruit fly's eye. A hexagonal grid of ommatidia/cartridges is shown with circles. Dashed circles indicate cartridges and solid circles indicate ommatidia. Note that ommatidia and cartridges are shown on the same plane only for compactness of illustration. Individual photoreceptors R1-R6 are numbered and their relative position highlighted in some of the ommatidia. Cartridge A receives 6 photoreceptor inputs, each from a different ommatidium. The arrows indicate the 6 photoreceptors that project to the target cartridge A. On the right, 6 photoreceptors from a single ommatidium each projects to a different cartridge. It is clear from the color code that the relative position between the ommatidia is always the same. For example, the location where the R3 cell (blue) resides and the cartridge where R3 projects to is locally always the same. Therefore, such a projection pattern tiles the visual space. (Adapted from [21].)

to the photoreceptors and have many inputs to the β-profiles generated by the T1 neurons [13] (see also Fig. 4). We assign 6 elements $\alpha 1$-$\alpha 6$ as the α-profiles in a cartridge. Note that these are not real neurons but serve as a link between Amacrine cells and the columnar neurons in the cartridge. α-profiles of the Am cells also feedback onto the photoreceptor input axons [18, 22].

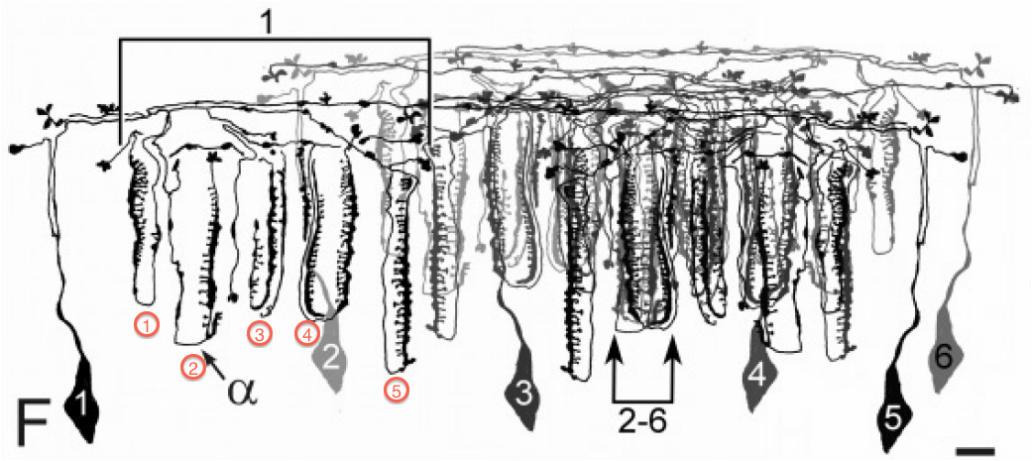

Figure 3: Anatomical structure of Amacrine cells. Cell 1 (indicated with number in the cell body) shows a partial reconstruction of an Amacrine cell that supplies one or two α-profiles to each of five cartridges (under bracket 1, each cartridge is numbered with a circle.). Cells $2-6$ are identical copies of cell 1. They provide the cartridge (indicated by arrowed bracket $2-6$) 6 α-profiles. Modified from [23], Copyright ©Cambridge University Press 2011.

The neurons/elements described above appear once in every cartridge; they are called *columnar neurons/elements*. Not all the neurons in the Lamina are columnar neurons, however. For example, the Lawf and Lat neurons are not associated with individual cartridges. Neurons in the Lamina that are not part of the repetitive structure of cartridges are referred to as *non-columnar neurons*. The overall cellular organization of columnar elements of a single cartridge is shown in Fig. 4. This figure illustrates a cross-section of the cartridge.

Connectivity The overall connectivity between neurons/elements in a single cartridge has been identified and can be summarized by the connectivity matrix in Table 3 [4].

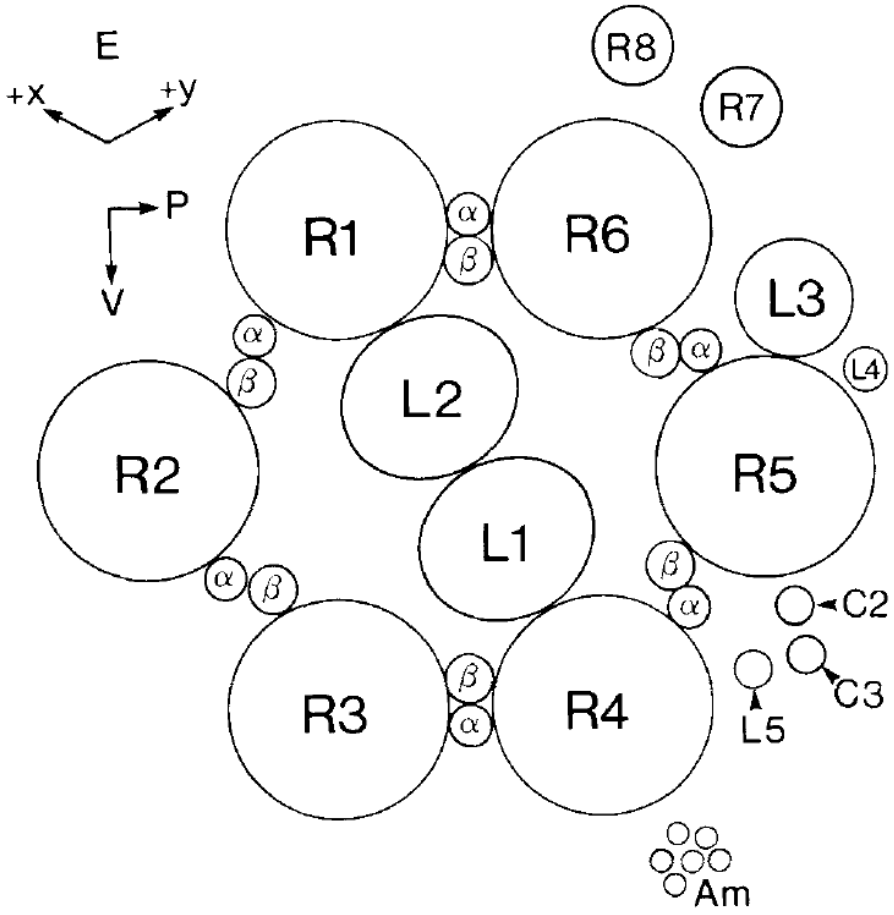

Figure 4: The position of elements in the cross section of a single cartridge. α-profiles from Amacrine cells and β-profiles from a T1 neuron can be seen in between each pair of adjacent photoreceptor axons. (From [13], Copyright ©1991 Wiley-Liss, Inc.)

Table 3: Number of synapses between neural elements in a single cartridge. (Empty means no connection, modified from [4])

Post \ Pre	R1	R2	R3	R4	R5	R6	L1	L2	L3	L4	L5	T1	C2	C3	α1	α2	α3	α4	α5	α6
R1								1												
R2								1								1				
R3																				
R4																	1	1		
R5										1								1	1	
R6																				
L1	40	43	37	38	38	45		3						3						
L2	46	45	39	41	39	47				2			3	5						
L3	11	10	4	8	6	12									1	1	1	3	5	1
L4						2		4										1	3	
L5								1										4		
T1		2	2	2											8	6	7	12	3	13
C2					1		5										1			
C3			2				3									1				
α1	19	16											1	1						
α2		22	18											3						
α3			20	16									2	2						
α4				17	26									2						
α5					10	14							1	2						
α6	17					22							1	3						

Fig. 5 shows the circuit diagram of a cartridge and summarizes the neurons and their connectivity.

Remark 1. *Cartridge neurons are non-spiking. They very likely extensively communicate via electrical synapses. Similar to gap junctions in the C. elegans and in the vertebrate retina, these electrical synapses may play an important role in the cartridge circuit. However, the data about them is scarce. We will ignore gap junctions in our Lamina model but they can be added as soon as data about them becomes available.*

Remark 2. *Recent connectome data reveals that more types of Medulla neurons may be presynaptic to the Lamina cartridge neurons [24]. For example, L1 may receive inputs from Mi1 and Tm3 cells, and those inputs are received in the Medulla rather than in the Lamina. How such inputs affect the L1 neuron, such as the direction of propagation of membrane potential, is not clear. A better understanding of these effects is needed before considering them as possibly part of the Lamina model.*

4.2 Cartridge Composition Rules

Composition Rule I The majority of the local neurons in the lamina are the Amacrine (Am) cells, characterized by their tangential structure and thin processes (α-profiles) generated by them. Cartridges do not possess local neurons. However, as we have discussed above, 6 α-profiles innervate each cartridge. They may come from 1 to 6 Amacrine cells. Each Amacrine cell also innervates multiple cartridges. Therefore, they can both pool information from many cartridges as well as broadcast information back to them.

Composition Rule II The majority of the connectivity amongst cartridges is mediated by non-columnar neurons, but synapses directly between output neurons are also common. Most of such connections are mediated by the L4 neurons. Each L4 neuron sends collaterals to two adjacent cartridges, whose relative positions to the cartridge containing the L4 neuron are fixed [13, 4]. The collaterals have a few contacts, pre-synaptic or post-synaptic, with other output neurons. A geometric view of these connections is shown in Fig. 6. Arrows of different colors indicate the connection mediated by the collaterals of different neurons.

Composition Rule III Other non-columnar neurons include Lawf neurons and Lat neurons. Both are output neurons that may pool information from multiple cartridges. A few types of Lawf neurons were identified based either on their morphology, that is the number of cartridges they innervate, or on their immunoreactivity

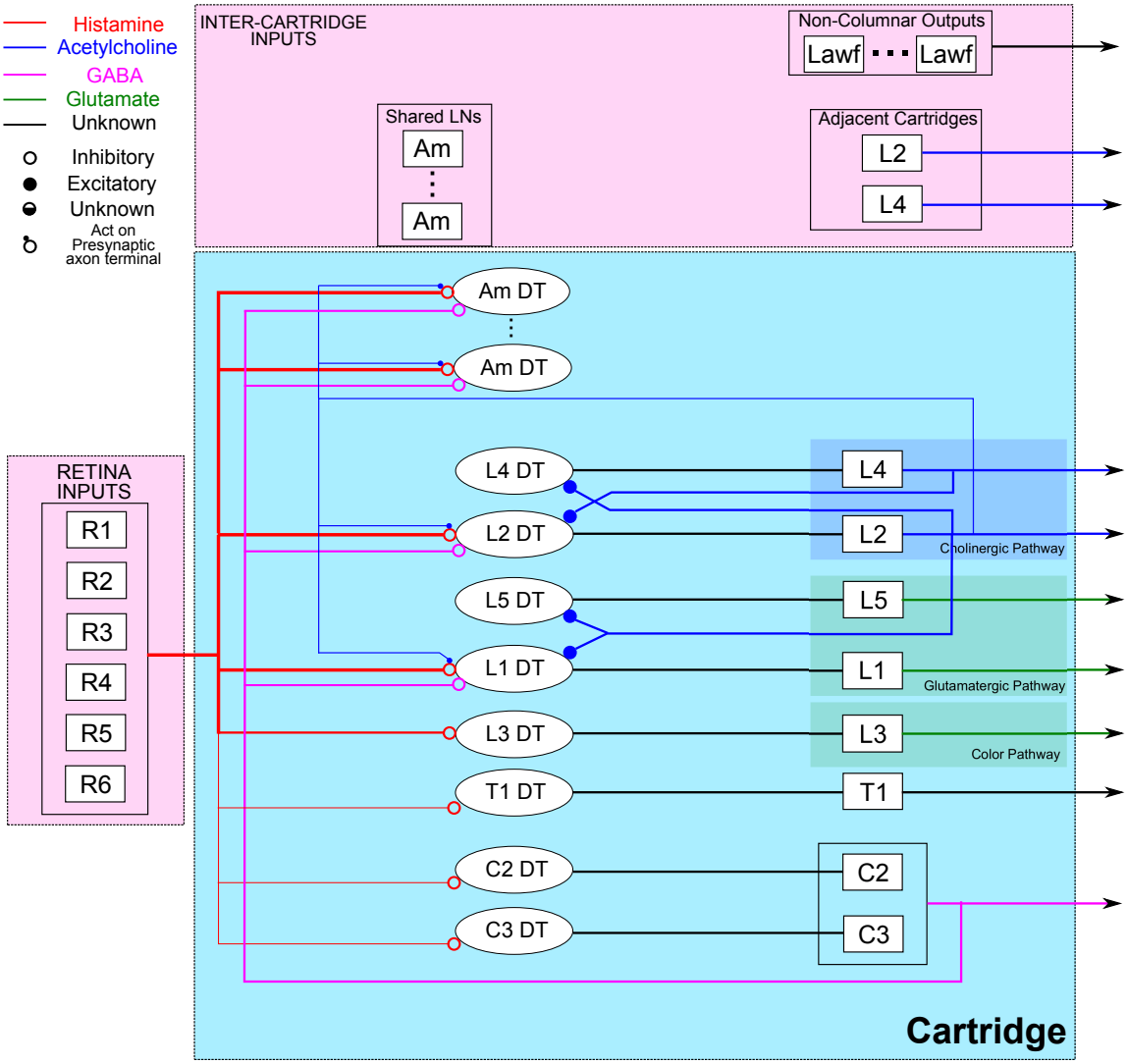

(a)

Figure 5: Block diagram of a cartridge (DT: Dendritic Tree). (a) Showing only intra-cartridge connections. Type of neurotransmitter is indicated by the color of the lines. Excitatory synapses are indicated by solid circles attached to DTs, and inhibitory synapses are indicated by empty circles. Smaller circles that are attached to larger circles indicate that the synapses act on axon terminals and therefore modulate the synaptic outputs of the other synapses. Lat neurons are omitted due to lack of data.

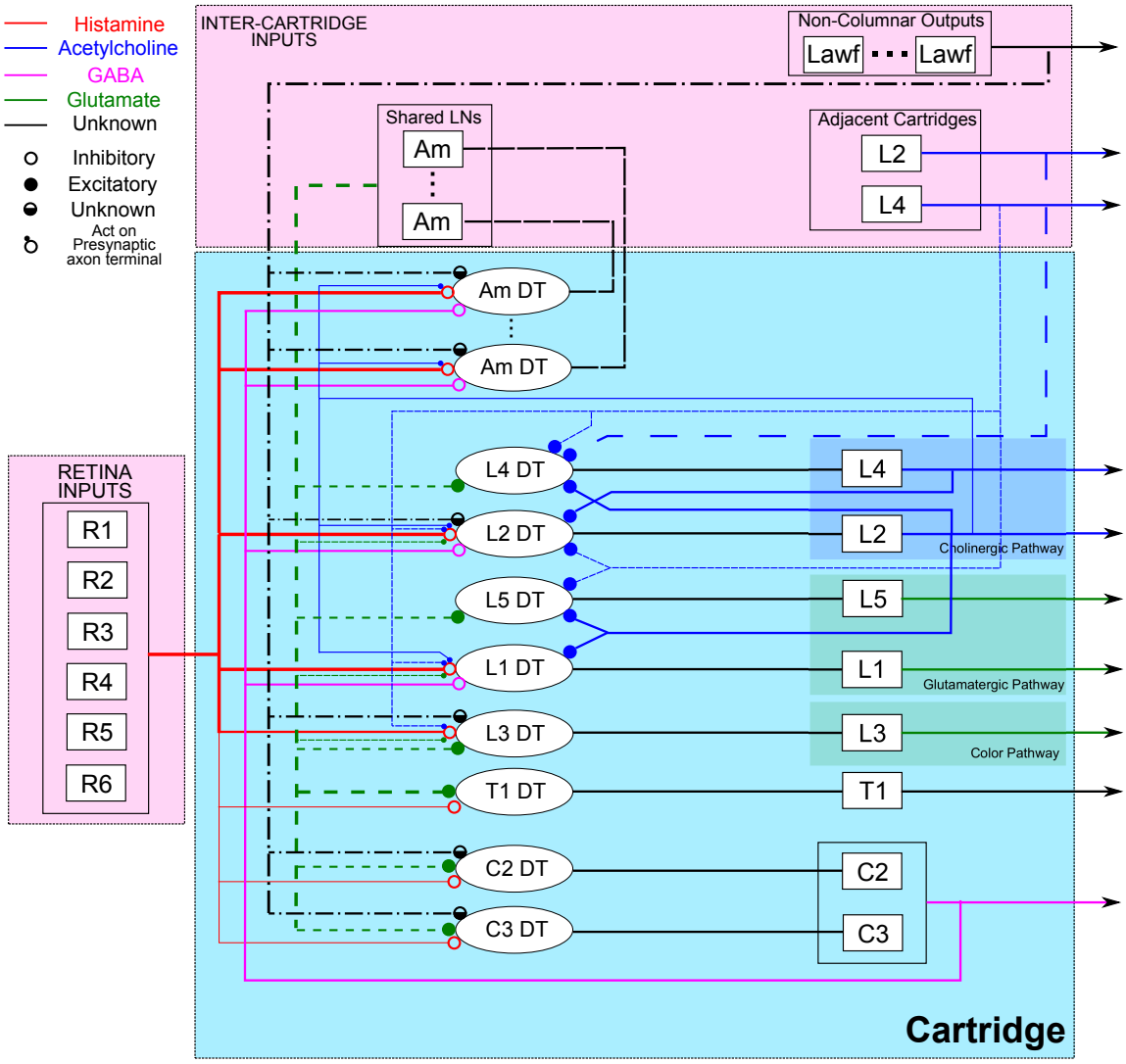

(b)

Figure 5: (Continued) Block diagram of a cartridge (DT: Dendritic Tree). (b) Showing both intra-cartridge connections (solid lines) and inputs from adjacent cartridges and non-columnar elements (dashed lines, see also Fig. 7). Lat neurons are omitted due to lack of data.

[3, 25].

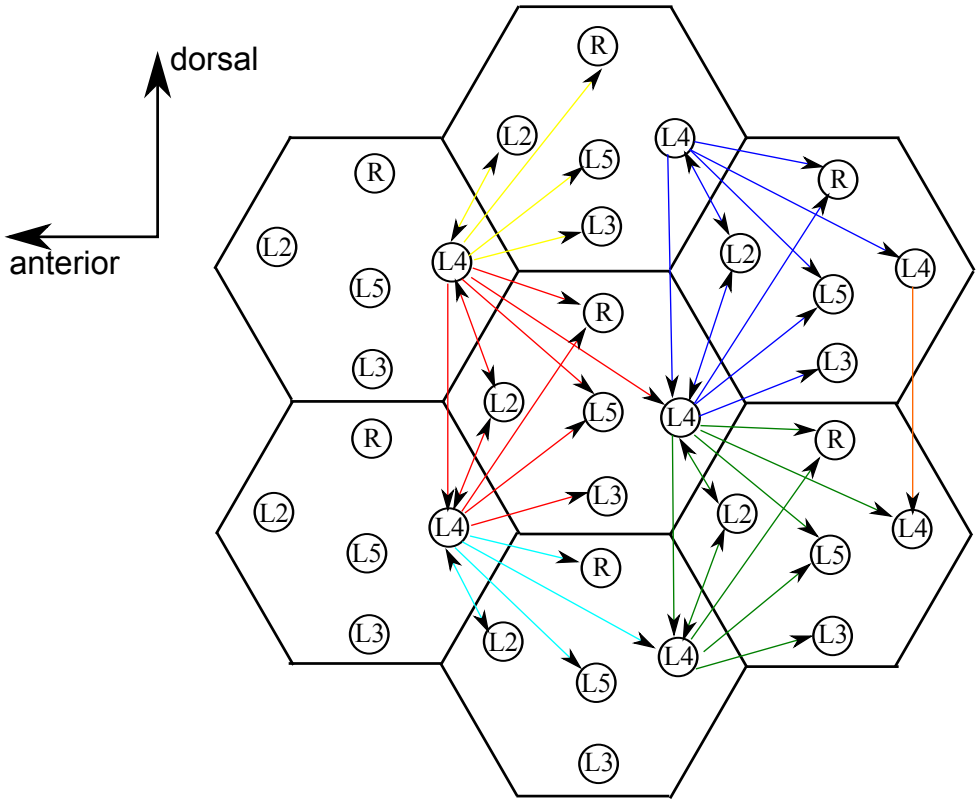

Figure 6: Inter-cartridge connectivity between cartridge output neurons. These connections are mediated by L4 collaterals from two adjacent cartridges. For example, the red arrows show the connections among the cartridge neurons in the very middle, and the cartridge neurons in the first column. The connections are each mediated by the two L4 neurons of the left cartridges that send collaterals to some of the neurons of the middle cartridge. The tiling of the visual space is extrapolated from data in a single cartridge. That is, for example, the blue and green arrows show the same pattern as the red arrows.

The composition of cartridges is summarized in Fig. 7. It shows that 3 adjacent cartridges are interconnected through the local neurons (green), L4 neurons (blue) as well as non-columnar output neurons (red), each representing one of the three composition rules.

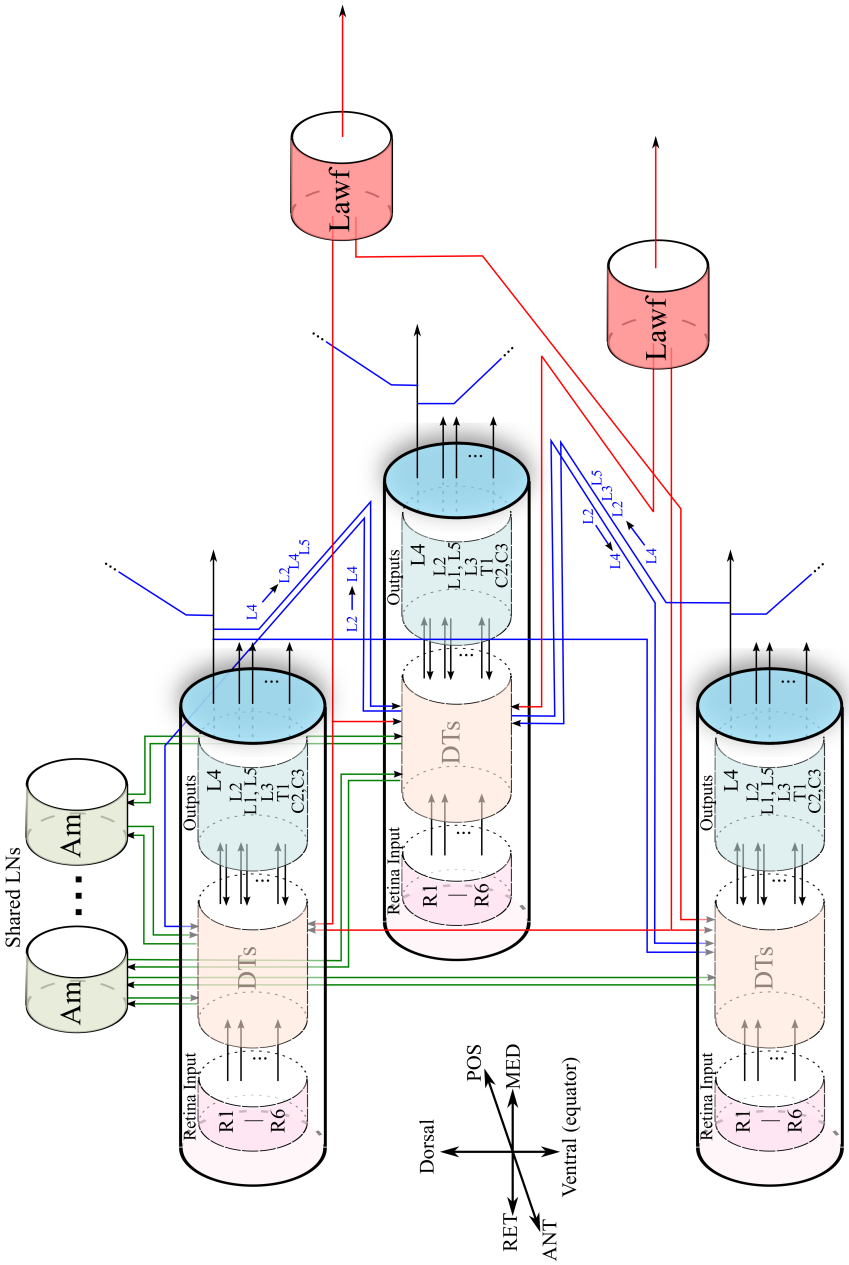

Figure 7: Overall structure of connections among cartridges. Connections in composition rule I are shown with green lines. Connections in composition rule II are shown with blue lines (The three cartridges here can be associated to the two cartridges in the first column and the middle cartridge in Fig. 6). Connections in composition rule III are shown with red lines. See also Fig. 5b.

5 Circuit Components and Implementation Considerations

5.1 Neuron Model

Since the Lamina consists of non-spiking neurons that only communicate through graded potential values, we decided to use a conductance based neuron model. For simplicity, we used a two-dimensional system that resembles the Morris-Lecar neuron model and picked parameters such that the model will not generate spikes. The description of the model is given by the systems of differential equations

$$\begin{aligned}\frac{dV}{dt} &= b - I_{syn} - g_L(V - E_L) - 0.5 g_{Ca}\left(1 + \tanh\left(\frac{V - V_1}{V_2}\right)\right)(V - E_{Ca}) - g_K n (V - E_K) \\ \frac{dn}{dt} &= \left(0.5\left(1 + \tanh\left(\frac{V - V_3}{V_4}\right)\right) - n\right)\left(\phi \cdot \cosh\left(\frac{V - V_3}{2V_4}\right)\right)\end{aligned} \tag{1}$$

where b is a preset constant bias current, $I_{syn} = I_{syn}(t)$ is the input synaptic current, $E_L = -50\text{mV}$, $E_{Ca} = 100\text{mV}$ and $E_K = -70\text{mV}$ are reverse potential values, and $g_L = 0.5$, $g_{Ca} = 2.0$ and $g_K = 1.1$ are maximum conductance values. Finally, V_1, V_2, V_3, V_4 and ϕ are the parameters to be tuned. In a more general setup, all the above parameters can be used to tune the neuron's response.

The tuning of the neuron's parameters can be performed in the phase space by altering the nullclines of the two variables, which can be expressed in closed form as (assuming input is zero)

$$\begin{aligned}\text{V nullcline: } n &= \frac{b - g_L(V - E_L) - 0.5 g_{Ca}\left(1 + \tanh\left(\frac{V - V_1}{V_2}\right)\right)(V - E_{Ca})}{g_K(V - E_K)} \\ \text{n nullcline: } n &= 0.5\left(1 + \tanh\left(\frac{V - V_3}{V_4}\right)\right)\end{aligned} \tag{2}$$

An example of the nullclines is shown in Figure 8a and the corresponding neuron response to step pulses is shown in Figure 8b.

A more elaborate conductance model that may be useful in the future appears in [26].

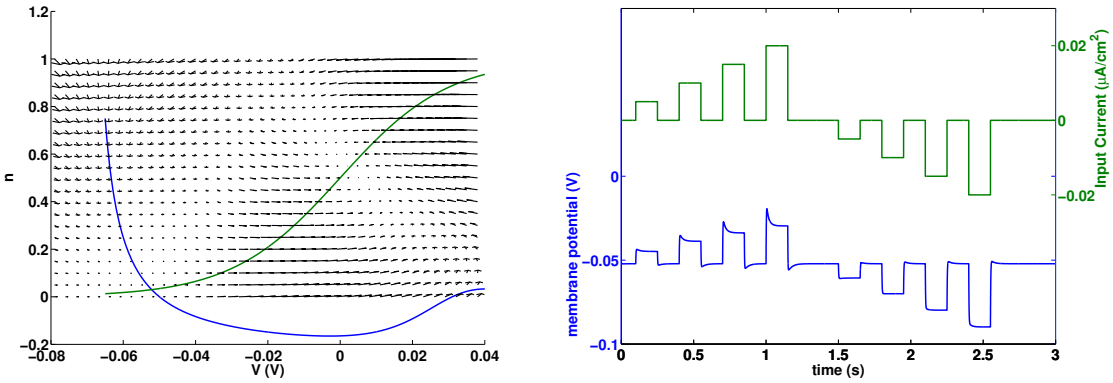

(a) (b)

Figure 8: (a) Example of nullclines in phase space, where blue curve is the V-nullcline and the green curve is the n-nullcline. (b) Step pulse response of the neuron whose nullclines are shown in (a). (green) input current (blue) membrane potential.

5.2 Synapse Model

For the chemical synapses that are activated by the graded potentials of non-spiking neurons, we used a simple model to capture the tonic release of neurotransmitter and its effect on the postsynaptic conductance. We defined a function that maps the presynaptic membrane potential to the postsynaptic conductance. The simplest form of such a function is described in Figure 9 and can be expressed as

$$g(t) = \min(g_{sat}, k(\max((V_{pre}(t - t_{delay}) - V_{th})^n, 0)), \tag{3}$$

where V_{pre} is the membrane potential of the presynaptic neuron and g_{sat}, V_{th}, k, n are tunable parameters representing the saturation of conductance, threshold, scale and power, repsectively. A configurable synaptic delay t_{delay} is added to each synapse. The role of this parameter is to approximate the disparate time scales involved in the synaptic release of various neurotransmitters.

The synaptic current can then be determined by

$$I_{syn}(t) = g(t)(V_{post}(t) - V_{rev}), \tag{4}$$

where V_{post} and V_{rev} are the membrane potential of the postsynaptic neuron and the reverse potential associated with the neurotransmitter. Whether the synapse is excitatory or inhibitory can be determined by the difference between V_{post} and

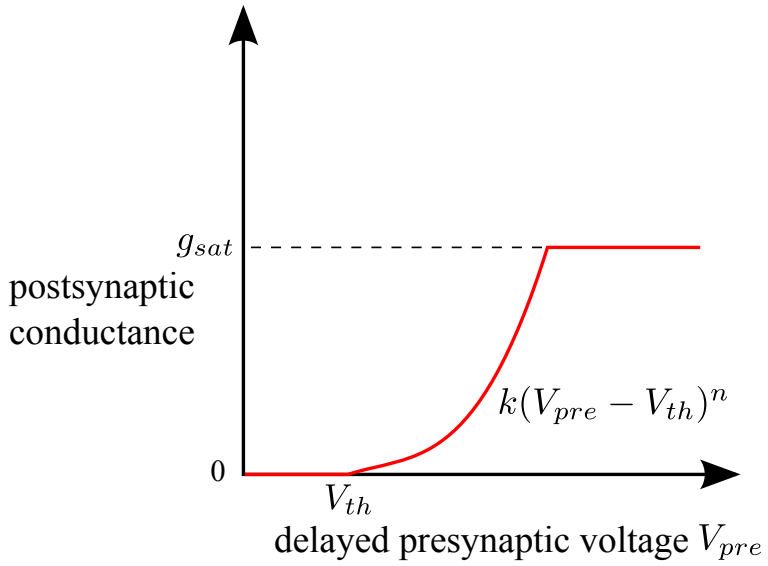

Figure 9: Model of synaptic transmission from a chemical synapse of a non-spiking neuron. The model takes the delayed membrane potential of the presynaptic neuron and maps it to a postsynaptic conductance. The function can be characterized based on the threshold, saturation, a scale variable, the power and the time delay.

V_{rev}. Since the synaptic current will affect the first equation of the neuron, if V_{post} is smaller than V_{rev}, the synapse is excitatory, and vice versa.

The reversal potential is set according to

a) The available data regarding the identified or hypothesized neurotransmitter/receptor pair,

b) The polarity of synapse should match recorded responses of cell types, if available. For example, LMCs should hyperpolarize to light increments.

5.3 Configuration of the Lamina Neural Circuit Model

The neuron and synapse models were implemented as part of? a Neurokernel LPU class; these were initially designed and verified for the Lamina circuit realization. The Neurokernel LPU class implements GPU-level execution of the LPU models. Consequently, we only provide here a configuration of the Lamina LPU to instantiate it in Neurokernel. The Lamina LPU configuration is based on the cartridge model

defined in Section 4.

Cartridges are defined on a hexagonal grid on a 2D plane, as shown on Fig. 10. Each cartridge then has a coordinate associated with it. Adjacent cartridges can be easily located with their unique coordinates.

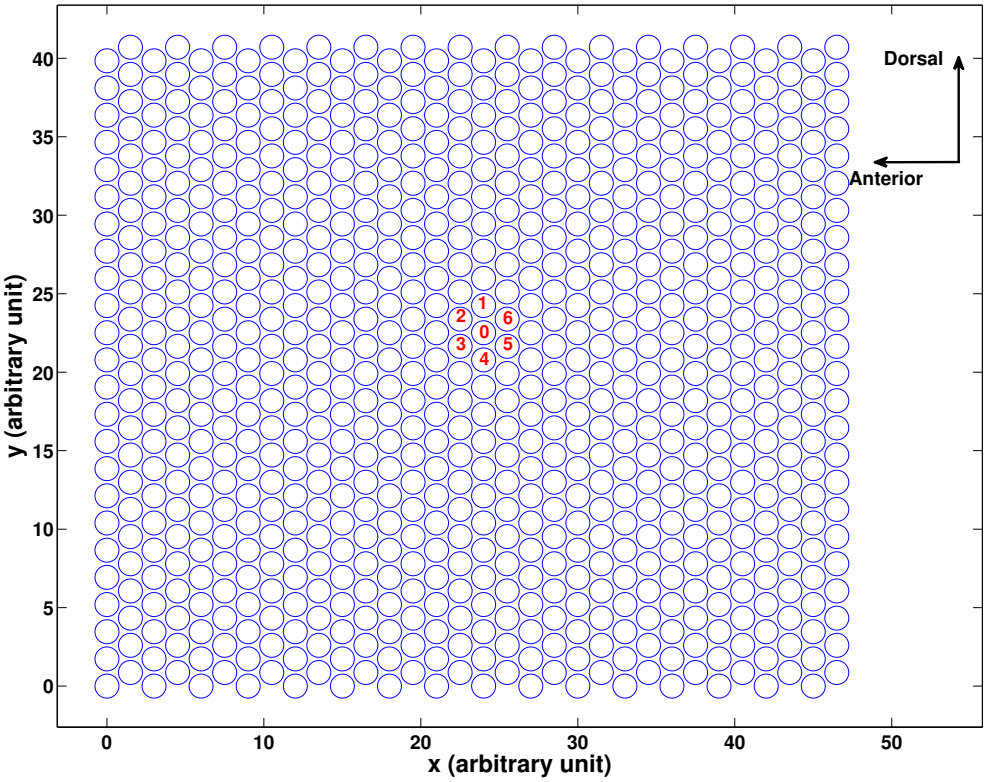

Figure 10: Hexagonal grid organization of a cross section of the Lamina cartridges on a 2D plane (right eye). Each circle represents a cartridge. Anterior and Dorsal direction are indicated, and distal direction is into the paper sheet. See also the coordinate system in Fig. 6 and 7.

All the neural elements in the Lamina LPU are listed in a CSV file [27], as shown in Table 4. This includes: output neurons L1-L5, T1, C2 and C3 neurons and local neuron Am. Due to lack of data, we did not include in the current implementation the Lawf and Lat neurons. We expect to include them as soon as more data on these becomes available. In addition, 6 α-profiles are included in each cartridge, named α1-α6 (see also Section 4.1, Local Neurons).

Table 4: Example CSV file showing the configuration of the neural elements. Column 'C' indicates whether the neuron is columnar or not, column 'D' indicates whether it is a dummy element (Am profiles), columns 'I' and 'O' indicates if the element is postsynaptic to input axons and if it is an output neuron, respectively. The rest of the columns display the parameters of equation (1)

Type	C	D	I	O	V_1	V_2	V_3	V_4	ϕ	$V(0)$	$n(0)$	b
L1	1	0	1	1	-0.001	0.015	-0.05	0.001	0.0025	-0.05	0.5	0.02
L2	1	0	1	1	-0.001	0.015	-0.05	0.001	0.0025	-0.05	0.5	0.02
L3	1	0	1	1	-0.001	0.015	-0.05	0.001	0.0025	-0.05	0.5	0.02
L4	1	0	0	1	-0.001	0.015	-0.05	0.001	0.0025	-0.05	0.5	0.02
L5	1	0	0	1	-0.001	0.015	-0.05	0.001	0.0025	-0.05	0.5	0.02
T1	1	0	1	1	-0.001	0.015	-0.05	0.001	0.0025	-0.05	0.5	0.02
C2	1	0	1	1	-0.001	0.015	-0.05	0.001	0.0025	-0.05	0.5	0.02
C3	1	0	1	1	-0.001	0.015	-0.05	0.001	0.0025	-0.05	0.5	0.02
Am	0	0	1	0	-0.001	0.015	0	0.03	0.2	-0.05184	0.0306	0
$\alpha 1$	1	1	1	0	-0.001	0.015	-0.05	0.001	0.0025	0	0	0
$\alpha 2$	1	1	1	0	-0.001	0.015	-0.05	0.001	0.0025	0	0	0
$\alpha 3$	1	1	1	0	-0.001	0.015	-0.05	0.001	0.0025	0	0	0
$\alpha 4$	1	1	1	0	-0.001	0.015	-0.05	0.001	0.0025	0	0	0
$\alpha 5$	1	1	1	0	-0.001	0.015	-0.05	0.001	0.0025	0	0	0
$\alpha 6$	1	1	1	0	-0.001	0.015	-0.05	0.001	0.0025	0	0	0

Synapses are listed in a separate CSV file that includes connections between columnar elements and interconnections between cartridges. Connections between columnar elements in a cartridge are set according to Table 3. If one neuron has more than one synaptic contact with another, it is registered as a single synapse, but the weight of the synapse is multiplied by the number of actual synaptic contacts. This is a first modeling approximation of multiple synapses between a pair of neurons. An example CSV file is tabulated in Table 5.

Table 5: Example CSV file showing the configuration of synapses. Column 'Pre' indicates the presynaptic neuron type. Column 'Post' indicates the postsynaptic neuron type. Column 'Cartridge' indicates the cartridge number relative to the cartridge containing the presynaptic element. For example, '0' indicates that the connection from R1 to L1 is in the same cartridge, and '1' to '6' identifies one of the immediate neighbors in the hexagonal grid (see also Figure 10). Column '# of synapses' indicates the actual number of synapses between the pre- and post-synaptic neurons. Column 'mode' indicates if synapses act on the axon terminal of the postsynaptic element (value 1) or the dendrite of the postsynaptic element (value 0). The rest of the columns are the parameters in the equations (3) and (4).

Pre	Post	Cartridge	$V_{rev}(V)$	$t_{delay}(ms)$	$V_{th}(V)$	k	n	g_{sat}	# of synapses	mode
R1	L1	0	-0.08	1	-0.05214	0.02	1	0.0008	40	0
R2	L1	0	-0.08	1	-0.05214	0.02	1	0.0008	43	0
R3	L1	0	-0.08	1	-0.05214	0.02	1	0.0008	37	0
R4	L1	0	-0.08	1	-0.05214	0.02	1	0.0008	38	0
R5	L1	0	-0.08	1	-0.05214	0.02	1	0.0008	38	0
R6	L1	0	-0.08	1	-0.05214	0.02	1	0.0008	45	0
L2	R1	0	0	1	-0.0505	1	1	0.02	1	1
$\alpha 5$	L3	0	-0.7	1	-0.5284	0.05	1	0.01	5	0

The interconnection of cartridges is based on the composition rules. They are discussed next.

First, composition Rule I calls for the interconnection of cartridges with a total of 300 Amacrine cells. These cells have α-profiles innervating multiple cartridges in a certain area. Each Amacrine cell is assigned a coordinate in the 2D plane; this coordinate is chosen from a uniform distribution inside the span of all the cartridges. Then, each α-profile in a cartridge is assigned to an Amacrine cell. The assignment is chosen at random from all the Amacrine cells that are within a certain distance from the cartridge where the α-profile resides. Finally, since α-profiles are now part of assigned Amacrine cells, the synapses defined previously between $\alpha 1$ to $\alpha 6$ and other neurons are transferred to become synapses between the corresponding Amacrine cells and other neurons. For example, the last row in Table 5 now describes the synapse between an Am cell and an L3 neuron, where the Am is the assigned neuron to $\alpha 5$.

Second, interconnections mediated by L4 neurons are setup between adjacent cartridges. Such interconnections are configured based on the composition Rule II. Since this composition rule applies to every cartridge, all connections can be defined using the CSV file again. An example is given by Table 6.

Table 6: Example CSV file showing the configuration of synapses between cartridges. Column 'Pre' indicates the presynaptic neuron type. Column 'Post' indicates the postsynaptic neuron type. Column 'Cartridge' indicates the cartridge number relative to the cartridge with the presynaptic element. For example, '0' indicates the connection from R1 to L1 is in the same cartridge, and '1' to '6' indicates one of the immediate neighbors in the hexagonal grid (see also Figure 10). Column '# of synapses' indicates the actual number of synapses between the pre- and post-synaptic neurons. Column 'mode' indicates if the synapse acts on the axon terminal of the postsynaptic element (value 1) or the dendrite of the postsynaptic element (value 0). The rest of the columns show the parameters in the equations (3) and (4).

Pre	Post	Cartridge	$V_{rev}(V)$	$t_{delay}(ms)$	$V_{th}(V)$	k	n	g_{sat}	# of synapses	mode
L2	L4	2	0	1	-0.0505	2	1	0.03	4	0
L2	L4	3	0	1	-0.0505	2	1	0.03	2	0
L4	L4	4	0	1	-0.0505	2	1	0.05	2	0
L4	R3	5	0	1	-0.0505	2	1	0.1	2	1
L4	L4	5	0	1	-0.0505	2	1	0.05	1	0
L4	L2	6	0	1	-0.0505	0.5	1	0.2	3	0

Due to lack of data for the Lawf and Lat neurons, the composition Rule III was omitted from the current implementation. We expect to include these neurons in a future implementation as soon as more data becomes available.

The configuration of the entire Lamina LPU with N cartridges is then populated from the single cartridge configuration and the composition rules employed. We used $N = 768$ cartridges in total. The Lamina LPU currently consists of $6,444$ neurons, the axon of $4,608$ input neurons and some $70,000$ synapses.

6 Acknowledgements

The research reported here was supported by AFOSR under grant #FA9550-12-1-0232.

References

[1] Ann-Shyn Chiang, Chih-Yung Lin, Chao-Chun Chuang, Hsiu-Ming Chang, Chang-Huain Hsieh, Chang-Wei Yeh, Chi-Tin Shih, Jian-Jheng Wu, Guo-Tzau Wang, and Yung-Chang Chen. Three-dimensional reconstruction of brain-wide wiring networks in Drosophila at single-cell resolution. Current Biology, 21(1):1–11, January 2011.

[2] Lev E. Givon and Aurel A. Lazar. Neurokernel: An open scalable software framework for emulation and validation of Drosophila brain models on multiple GPUs. submitted for publication, 2013.

[3] K.-F. Fischbach and A. P. M. Dittrich. The optic lobe of Drosophila melanogaster. I. A Golgi analysis of wild-type structure. Cell Tissue Research, 258:441–475, 1989.

[4] Marta Rivera-Alba, Shiv N. Vitaladevuni, Yuriy Mischenko, Zhiyuan Lu, Shin-ya Takemura, Lou Scheffer, Ian A. Meinertzhagen, Dmitri B. Chklovskii, and Gonzalo G. de Polavieja. Wiring economy and volume exclusion determine neuronal placement in the Drosophila brain. Current Biology, 2011. doi:10.1016/j.cub.2011.10.022.

[5] Shin-ya Takemura, Zhiyuan Lu, and Ian A. Meinertzhagen. Synaptic circuits of the Drosophila optic lobe: The input terminals to the medulla. The Journal of Comparative Neurology, 509:493–513, 2008.

[6] Shamprasad Varija Raghu and Alexander Borst. Candidate glutamatergic neurons in the visual system of Drosophila. PLoS One, 6(5):e19472, 2011.

[7] Shamprasad Varija Raghu, Jing Claussen, and Alexander Borst. Neurons with cholinergic phenotype in the visual system of Drosophila. Journal of Comparative Neurology, 519:162–176, 2011.

[8] Shamprasad Varija Raghu, Jing Claussen, and Alexander Borst. Neurons with GABAergic phenotype in the visual system of Drosophila. Journal of Comparative Neurology, 521:252–265, 2013.

[9] Marion Silies, Dary M. Gohl, Yvette E. Fisher, Limor Freifeld, Damon A. Clark, and Thomas R. Clandinin. Modular use of peripheral input channels tunes motion-detecting circuitry. Neuron, 79:111–127, 2013.

[10] Aurel A. Lazar, Wenze Li, Nikul H. Ukani, Chung-Heng Yeh, and Yiyin Zhou.

Neural circuit abstractions in the fruit fly brain. Society for Neuroscience Abstracts, 2013.

[11] Alois Hofbauer and José A. Campos-Ortega. Proliferation pattern and ealry differentiation of the optic lobes in Drosophila melanogaster. Roux's Archives of Developmental Biology, 198:264–274, 1990.

[12] Nicholas J. Strausfeld. The organization of the insect visual system (light microscopy) i. projections and arrangement of neurons in the lamina ganglionaris of diptera. Zeitschrift für Zellforschung und Mikroskopische Anatomie, 121:377–441, 1971.

[13] I. A. Meinertzhagen and S. D. O'Neil. Synaptic organization of columnar elements in the lamina of the wild type in Drosophila melanogaster. The Journal of Comparative Neurology, 305:232–263, 1991.

[14] Alexander Borst. Drosophila's view on insect vision. Current Biology, 19, 2009. doi:10.1016/j.cub.2008.11.001.

[15] Roger C. Hardie. A histamine-activated chloride channel involved in neurotransmission at the photoreceptor synapse. Nature, 339:704–706, 1989.

[16] Shin-ya Takemura, Thangavel Karuppudurai, Chun-Yuan Ting, Zhiyuan Lu, Chi-Hon Lee, and Ian A. Meinertzhagen. Cholinergic circuits integrate neighboring visual signals in a Drosophila motion detection pathway. Current Biology, 21:2077–2084, 2011.

[17] Nicol D. and Meinertzhagen I. A. An analysis of the number and composition of the synaptic populations formed by photoreceptors of the fly. Journal of Comparative Neurology, 207(1):29–44, 1982.

[18] Lei Zheng, Gonzalo G. de Polavieja, Verena Wolfram, Musa H. Asyalia, Roger C. Hardie, and Mikko Juusola. Feedback network controls photoreceptor output at the layer of first visual synapses in drosophila. The Journal of General Physiology, 127(5):495–510, 2006.

[19] Antonios Pantazis, Ashvina Segaran, Che-Hsiung Liu, Anton Nikolaev, Jens Rister, Andreas S. Thum, Thomas Roeder, Eugene Semenov, Mikko Juusola, and Roger C. Hardie. Distinct roles for two histamine receptores (hclA and hclB) at the Drosophila photoreceptor synapse. Journal of Neuroscience, 28(29):7250–7259, 2008.

[20] Dmitri B. Chklovskii, Shiv Vitaladevuni, and Louis K. Scheffer. Semi-automated

reconstruction of neural circuits using electron microscopy. Current Opinion in Neurobiology, 20:667–675, 2010.

[21] Kuno Kirschfeld. Die projektion der optischen umwelt auf das raster der rhabdomere im komplex auge von musca. Experimental Brain Research, 3:248–270, 1967.

[22] Joshua R Sanes and S Lawrence Zipursky. Design principles of insect and vertebrate visual systems. Neuron, 66(1):15–36, 2010.

[23] John K. Douglass and Nicholas J. Strausfeld. Sign-conserving amacrine neurons in the fly's external plexiform layer. Visual Neuroscience, 22:345–358, 2005.

[24] Shin-ya Takemura, Arjun Bharioke, Zhiyuan Lu, Aljoscha Nern, Shiv Vitaladevuni, Patricia K. Rivlin, William T. Katz, Donald J. Olbris, Stephen M. Plaza, Philip Winston, Ting Zhao, Jane Anne Horne, Richard D. Fetter, Satoko Takemura, Katerina Blazek, Lei-Ann Chang, Omotara Ogundeyi, Mathew A. Saunders, Victor Shaprio, Christopher Sigmund, Gerald M. Rubin, Louis K. Scheffer, Ian A. Meinertzhagen, and Dmitri B. Chklovskii. A visual motion detection circuit suggested by Drosophila connectomics. Nature, 500:175–181, 2013.

[25] Agata Kolodziejczyk, Xuejun Sun, Ian A. Meinertzhagen, and Dick R. Nässel. Glutamate, GABA and acetylcholine signaling components in the lamina of the Drosophila visual system. PLoS One, 3(5):e2110, 2008. doi:10.1371/journal.pone.0002110.

[26] Zhuoyi Song, Daniel Coca, Stephen Billing, Marten Postma, Roger C. Hardie, and Mikko Juusola. Biophysical modeling of a Drosophila photoreceptor. ICONIP 2009, Part I, LNCS 5863, pages 57–71, 2009.

[27] Y. Shafranovich. Network working group request for comments: 4180, 2005.